



Low Relaxation Rate in Epitaxial Vanadium-Doped Ultrathin Iron Films

C. Scheck,¹ L. Cheng,¹ I. Barsukov,² Z. Frait,² and W. E. Bailey^{1,*}

¹*Materials Science, Department of Applied Physics and Applied Mathematics, Columbia University, New York, New York 10027, USA*

²*Institute of Physics, Academy of Sciences of the Czech Republic, Prague, Czech Republic*

(Received 29 December 2006; published 12 March 2007)

The longest relaxation time and sharpest frequency content in ferromagnetic precession is determined by the intrinsic (Gilbert) relaxation rate G . For many years, pure iron (Fe) has had the lowest known value of $G = 57$ MHz for all pure ferromagnetic metals or binary alloys. We show that an epitaxial iron alloy with vanadium (V) possesses values of G which are significantly reduced to 35 ± 5 MHz at 27% V. The result can be understood as the role of spin-orbit coupling in generating relaxation, reduced through the atomic number Z .

DOI: 10.1103/PhysRevLett.98.117601

PACS numbers: 76.30.Fc, 72.25.Rb, 75.40.Gb, 75.50.Bb

Ultrafast magnetization dynamics comprise a major area of current research in magnetism. Novel dynamical phenomena have been observed recently in confined structures [1], with programmed field pulses [2,3], through interactions with intense light pulses [4,5], and under the influence of spin polarized currents [6,7].

In all cases, the observed phenomena compete against ferromagnetic relaxation in the magnetic material. Relaxation aligns magnetization \mathbf{M} with applied fields \mathbf{H} , bringing dynamics to a stop. The lowest limit of the relaxation rate is intrinsic to a given material and given by $G = \gamma\alpha M_s$, where α is the related dimensionless damping constant. In metals, the damping has seen renewed theoretical interest [8] motivated particularly by its formal relationship with spin momentum transfer torques [9,10], or by its enhancement with impurities [11]. Low relaxation rates are of particular interest for low critical currents in spin momentum transfer [12], narrow band response in frequency domain devices [13], and reduced thermal noise in nanoscale magnetoresistive sensors [14].

Pure iron (Fe) has long been known to exhibit the lowest measured intrinsic relaxation rate of all elemental ferromagnetic metals or binary alloys [15]. Lowest values of 57 MHz ($\alpha = 0.002$) have been found in both single-crystal whiskers and epitaxial films [16] at room temperature. Elemental Ni, Co, and standard alloys such as $\text{Ni}_{81}\text{Fe}_{19}$ show much higher values ($G = 220, 170, 114 \pm 10$ MHz, respectively.)

In this Letter, we show that the intrinsic relaxation rate G in a low- Z ferromagnetic alloy can be substantially lower than that known for pure Fe. Epitaxial $\text{MgO}(100)/\text{Fe}_{1-x}\text{V}_x(8\text{ nm})(100)$ ultrathin films, deposited by UHV sputtering, exhibit values of G to 35 MHz, reduced by $\sim 40\%$. While a comparable value has been identified recently in NiMnSb [7], the low damping has been attributed to the special electronic characteristics of this ordered, half-metallic compound [17], including a low orbital component of the magnetic moment. We show that in $\text{Fe}_{1-x}\text{V}_x$ the observed effect can be understood as the reduced

influence of spin-orbit coupling in lighter ferromagnets, pervasive across the $3d$ series.

The intrinsic (or Gilbert) relaxation rate G is defined in the Landau-Lifshitz-Gilbert equation for magnetization dynamics (cgs units):

$$\frac{\partial \mathbf{M}}{\partial t} = -|\gamma| \mathbf{M} \times \mathbf{H}_{\text{eff}} + \frac{G}{\gamma M_s^2} \mathbf{M} \times \frac{\partial \mathbf{M}}{\partial t}, \quad (1)$$

where $\mathbf{H}_{\text{eff}} = \mathbf{H}_{\text{ext}} + \mathbf{H}_{\mathbf{K}} + \mathbf{H}_{\text{demag}}$ is the effective field with external, anisotropy, and demagnetization components and $\gamma = g_{\text{eff}}(e/2mc) = (g_{\text{eff}}/2) \times 17.588$ MHz/Oe is the gyromagnetic ratio, with g_{eff} the spectroscopic factor. Equation (1) can be solved for power absorption in transverse rf susceptibility, as performed in a ferromagnetic resonance (FMR) measurement. Damping α is measured through variable-frequency FMR linewidth as

$$\Delta H_{pp} = \Delta H_0 + \frac{2}{\sqrt{3}} \frac{\alpha}{\gamma} 2\pi f, \quad (2)$$

where ΔH_{pp} is the field-swept FMR peak-to-peak linewidth, ΔH_0 is the inhomogeneous (extrinsic) broadening, and f is the microwave frequency. Extrinsic losses are thought to be entirely microstructure-related, and (in principle) possible to reduce through optimized microstructure. G is derived from measurements of α .

In our experiments, α is measured in variable-frequency, field-swept FMR using four separate shorted rectangular waveguide assemblies at 17, 25, 49, and 70 GHz, with 2 mm iris; see [16] for details. Frequency-swept FMR measurements were carried out using a synthesized microwave sweep generator operating in cw mode over the range 9–40 GHz [13], with sample mounted on a broadband coplanar waveguide, over an exciting area of 0.1 mm^2 ; an identical setup was used for the identification of field-for-resonance $f(H_{\text{res}})$. All measurements were carried out at room temperature, with magnetization in the film plane, along $[110]\text{Fe}_{1-x}\text{V}_x/[100]\text{MgO}$ unless otherwise noted.

Two series of epitaxial $\text{MgO}(100)/\text{Fe}_{1-x}\text{V}_x(100)$ samples have been considered. A 50 nm series, to

52% V, was investigated for magnetic moment $4\pi M_s$ by vibrating sample magnetometry (VSM), magnetocrystalline anisotropy constant K_1 by rotation-controlled FMR in a X-band cavity, and spectroscopic factor g_{eff} by $f(H_{\text{res}})$ measurement. 8 nm samples have been compared between pure Fe and 27% V for Gilbert relaxation rate G ; ultrathin samples are necessary to exclude eddy current effects. This series had optimized, high rate deposition conditions for lowest G in pure Fe; the V composition of 27%, shown here, was the maximum attainable in our chamber for these conditions. Epitaxial structure was characterized in the 50 nm series using x-ray diffraction; intense (200) reflections, with narrow rocking curves $0.7\text{--}1.1^\circ$, were seen for the full compositional series $0 < x < 52\%$.

Figure 1 shows the variable-frequency, field-swept FMR data for 8 nm $\text{Fe}_{1-x}\text{V}_x$ alloy films, $x = 0$ and $x = 0.27$. We have determined α through a linear fit of $\Delta H(f)$ according to Eq. (2). For pure Fe, α is measured as 0.0019, in good agreement with the lowest measured values through exchange-conductivity analysis of single-crystal whiskers and sputtered epitaxial films with higher inhomogeneous loss [16]; the inhomogeneous loss ΔH_0 is 18 Oe. For $\text{Fe}_{1-x}\text{V}_x$, $x = 0.27$, we measure $\alpha = 0.0021$, with $\Delta H_0 = 28$ Oe.

Values of $4\pi M_s = 21.1$ and 11.6 kG, are measured for these 8 nm films, respectively, through perpendicular resonance (not shown). Calibrated VSM measurements (Fig. 3) for thicker (50 nm) films return values which are ~ 0.5 kG higher in each case, presumably due to some reduced moment at the surface for the thinner films. The observed reduction in the moment for the $\text{Fe}_{73}\text{V}_{27}$ alloy ($\sim 3.6\mu_B/\text{atom V}$) is close to the theoretical moment reduction from V impurities in Fe [18] ($\sim 3.4\mu_B/\text{atom V}$) and the Slater-Pauling value of $3.3\mu_B/\text{atom}$.

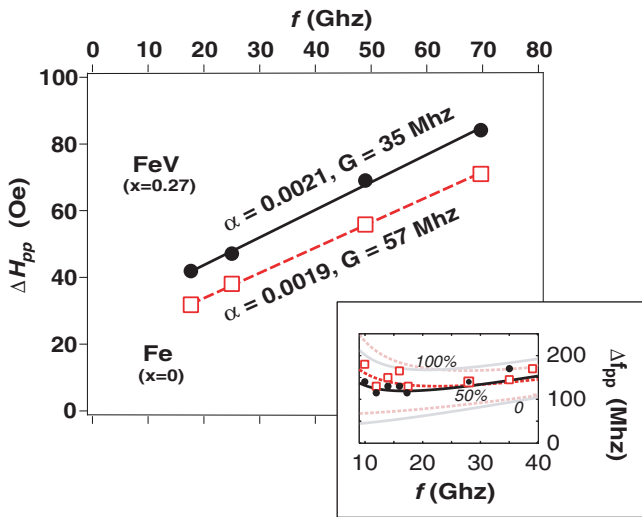


FIG. 1 (color online). Measurement of intrinsic damping parameter α and relaxation rate G in $\text{MgO}/\text{Fe}_{1-x}\text{V}_x$ (8 nm), $x = 0$ and 0.27 . Inset: swept-frequency FMR linewidths Δf ; lines show model calculations for different levels of inhomogeneous broadening.

The intrinsic relaxation rate G , combining experimental α and $4\pi M_s$ measurements of the thin films, is 57 ± 3 MHz for Fe and 35 ± 5 MHz for $\text{Fe}_{1-x}\text{V}_x$, $x = 0.27$. The reduction of G has a device-relevant manifestation. FMR frequency linewidths Δf at half-power (peak-to-peak) measure $2G$ ($2/\sqrt{3}G$) directly, in the low-frequency, intrinsic damping limit. Swept-frequency linewidths Δf_{pp} show lower values for the 27% V film by 15–30 MHz over the frequency range 10–18 GHz, as expected in analytical calculations assuming zero, 50%, and 100% of the swept-field measured inhomogeneous loss; calculations convert the field-swept linewidth ΔH to Δf by differentiating the Kittel relationship. Agreement is best for 50% (dark curve in Fig. 1); the reduced value of inhomogeneous broadening presumably reflects the smaller sampling area of the broadband technique.

We have also characterized the magnetocrystalline anisotropy in 50 nm $\text{Fe}_{1-x}\text{V}_x$ film series (Fig. 2.) The angular dependence of H_{res} exhibits a clear fourfold symmetry with minima along $[100]$ and $[0\bar{1}0]$ (easy axes) and maxima along $[110]$ and $[1\bar{1}0]$ (hard axes). As V concentration increases, the magnetocrystalline anisotropy is reduced to zero and negative values at $x \sim 0.44$ (inset). Numerical fits to extract the first cubic magnetocrystalline anisotropy constant K_1 were performed according to the method of Ref. [19]. Extracted values yield the expected value of 4.87×10^5 erg/cm³ for Fe; we find 1.29×10^5 erg/cm³ for $\text{Fe}_{73}\text{V}_{27}$. Data for $0 \leq x \leq 10\%$ match closely with the findings of Hall [18] to 15%; the nulling of K_1 at high x had not been identified previously.

The use of variable-frequency FMR measurement, with knowledge of $4\pi M_s$ values, allows the extraction of the gyromagnetic ratio g_{eff} , through the Kittel relation, $2\pi f = \gamma \sqrt{(H_B + 4\pi M_s + K_1/M_s)(H_B - 2K_1/M_s)}$, appropriate for film magnetization in-plane along $\langle 110 \rangle$. A plot of f^2 as a function of H_r , extracted from variable-frequency, field-swept FMR measurement of 50 nm films, is presented in Fig. 3. Values of $4\pi M_s$, taken from VSM measurements, were fixed in the fits; g_{eff} and K_1 were fit parameters.

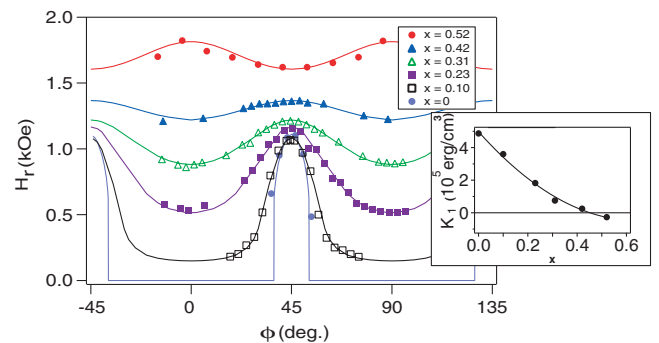


FIG. 2 (color online). Angular dependence of field-for-resonance H_{res} at 10 GHz, cavity measurement. Lines are fits to extract cubic anisotropy constants K_1 after [19]. Inset: K_1 values.

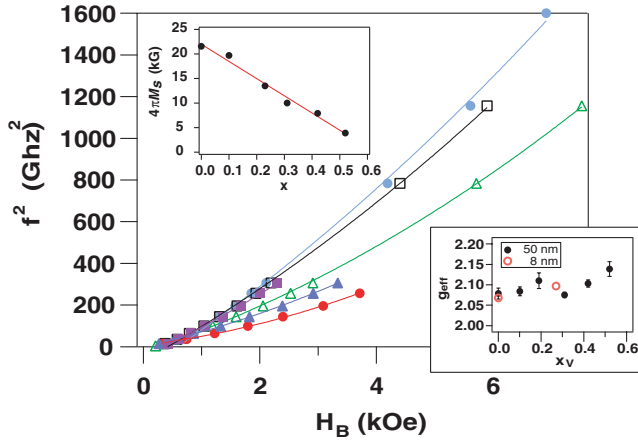


FIG. 3 (color online). Extraction of spectroscopic factor g_{eff} from variable-frequency FMR measurement, MgO/Fe $_{1-x}$ V $_x$ (8 and 50 nm) films. Inset, top left: VSM measurement of $4\pi M_s$. Inset, lower right: extracted g_{eff} values for 8 and 50 nm films.

Extracted K_1 values are in good agreement with those taken from rotational measurements.

Little change in g_{eff} is evident as the V concentration increases. g_{eff} values, shown in the inset of Fig. 3, are near 2.09 ± 0.02 for V composition up to 52%.

We have shown that Fe $_{1-x}$ V $_x$ alloys exhibit a reduction in intrinsic relaxation rate G . The magnetic moments of this alloy have been understood previously through a simple dependence on average electronic concentration Z , as seen in the well-known Slater-Pauling curve [18]. The VSM measurements of 50 nm films are presented together with the theoretical result in Fig. 4(a). $4\pi M_s$ data are also included from perpendicular FMR measurements of Cu-alloyed Ni $_{81}$ Fe $_{19}$, at $27.6 \leq Z \leq 28.0$, taken from Ref. [20]. Heusler alloy data, for NiMnSb [7] are included for comparison and plotted at $Z = 25$, as magnetic properties are thought to arise nearly entirely from moments localized to Mn sites [17].

In Fig. 4(c) we plot measurements of intrinsic relaxation rate G as a function of average electronic concentration Z . Data are taken from our measurements and collected from the literature. For consistency, we restrict ourselves to measurements of G in crystalline films, using variable-frequency FMR, in which the frequency-dependent change in (homogeneous) linewidth $1.158\Delta 2\pi f\alpha/\gamma$ exceeds the inhomogeneous linewidth ΔH_0 by at least a factor of 2. This requires 70 GHz measurements for Fe $_{1-x}$ V $_x$ (this work) and Fe $_{1-x}$ Co $_x$ [16] and 18 GHz measurements for Ni $_{81}$ Fe $_{19}$ and its alloys [20]. Lowest literature values are plotted; in, e.g., Fe, a dispersion of measured values from 57–140 MHz [7,21] has been attributed to variations in point defect density [22].

The data in Fig. 4(c) demonstrate a trend towards higher relaxation rate G at higher average valence Z . Values increase by a factor of 4, from 35 MHz for FeV (27%) to 150–220 MHz for (Ni $_{81}$ Fe $_{19}$) $_{0.7}$ Cu $_{0.3}$ and for pure Ni, respectively. Apart from the two pure metal points for Ni

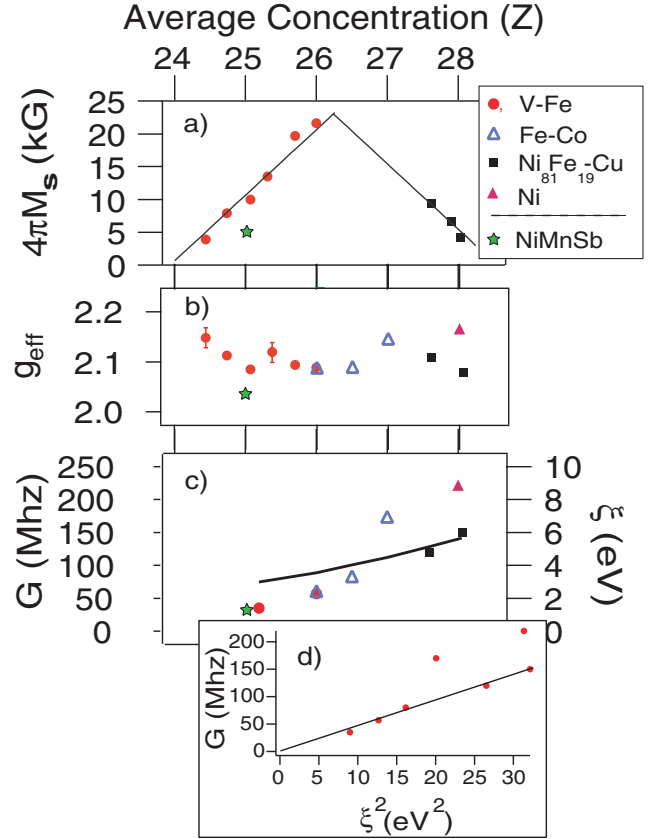


FIG. 4 (color online). Compositional dependence of (a) moment $4\pi M_s$, (b) gyromagnetic ratio g_{eff} , and (c) Gilbert relaxation rate G for $3d$ transition metal ferromagnetic substitutional alloys. Solid line: atomic spin-orbit coupling parameter ξ . (d) Relaxation G as a function of spin-orbit coupling ξ^2 . Data for FeV films, this work, for bcc or fcc Fe $_{1-x}$ Co $_x$, Ref. [16]; for Ni $_{81}$ Fe $_{19}$:Cu films, [20]; for Ni whiskers, [15]. The Heusler compound NiMnSb data [7] are included for comparison.

whiskers and the fcc Co film, there is a relatively smooth variation in the baseline formed by the alloys. For these species, there is no similar general trend in g_{eff} [Fig. 4(b)], measured constant at 2.10 ± 0.02 . Note that the NiMnSb point, of $G = 31$ MHz at $Z = 25$, is very close to our measurement of Fe $_{73}$ V $_{27}$ of 35 ± 5 MHz, even though g_{eff} is substantially lower (2.03 compared with 2.11).

As average concentration Z increases, so too does the expected spin-orbit coupling energy. Values for an effective atomic spin-orbit coupling parameter ξ , where $\hat{H}_{\text{so}} = \xi \sum_i \mathbf{l}_i \cdot \mathbf{s}_i$, have been tabulated in Ref. [23] for atomic $3d$ orbitals, in good agreement with atomic spectra. These values are reproduced here [Fig. 4(c), solid line]. In Fig. 4(d), we show the dependence of G on ξ , implicit in atomic number. It can be seen that the lower band of values is simply proportional to ξ^2 ; pure Ni and Co data points are significant outliers.

The observed scaling of Gilbert damping G with ξ^2 is in good agreement with electronic-scattering-based models of ferromagnetic relaxation, appropriate to metals [8]. Relaxation occurs as uniform-mode magnons are annih-

lated by one-electron spin-flip accelerations. The expression for relaxation rate G is given as [7]

$$G = \hbar\gamma^2\langle S \rangle^2 \xi^2 \int d^3\mathbf{k} \sum_{\alpha,\beta,\sigma} \langle \beta | L^+ | \alpha \rangle \langle \alpha | L^- | \beta \rangle \delta(E_{\alpha,\mathbf{k},\sigma} - E_{\beta,\mathbf{k},\sigma}) \frac{\hbar/\tau_M}{(\hbar\omega + E_{\alpha,\mathbf{k},\sigma} - E_{\beta,\mathbf{k},\sigma})^2 + (\hbar/\tau_M)^2},$$

where other leading materials parameters γ^2 and $\langle S \rangle^2 = (M(300\text{ K})/M(0\text{ K}))^2$ do not change by more than 5% or 10%, respectively, across the materials investigated. The second row terms describe the temperature dependence of relaxation through momentum scattering time τ_M , with a high-temperature limit $G \sim \tau_M^{-1} \sim T$, for scattering across spin sheets (“interband scattering”) and a low-temperature limit $G \sim \tau_M \sim 1/T$ for scattering within bands (“ordinary scattering”). The temperature dependence of G is known to be weak near 300 K for Fe, Co, Ni [15] and Ni₈₁Fe₁₉ [11], although it is not known with great precision except for Ni [7]. Thus it is not a gross distortion to take these terms as nearly constant, near 300 K, across the 3d series. The orbital moment terms, on the other hand, may not be constant: orbital moments do *not* follow a simple dependence upon Z in binary Fe, Co, Ni alloys [24], and the significantly larger values of $(g_{\text{eff}} - 2)^2$ observed for Co ($g_{\text{eff}} = 2.15$) and Ni ($g_{\text{eff}} = 2.17$) may help to explain their significantly higher values of G .

We do not expect that a universal proportionality between G and ξ^2 —a simple dependence upon Z —should exist. Deviations are noted for Ni and Co, materials with large g_{eff} . Ferromagnets with very large magnetostriction [25] are likely to be dominated by phonon drag mechanisms, weak in the materials under consideration here [26]. At low temperature and long scattering time τ_M the details of band structure, variable across the series, should become much more important [8]. Nevertheless, the scaling of relaxation rate G with spin-orbit coupling as ξ^2 provides a plausible interpretation for the very low relaxation rates seen in the low- Z alloy Fe_{1-x}V_x. It explains why similarly low values are seen in the very different Heusler compound NiMnSb. Finally, we hope that it will provide some guidance in the search for ferromagnets with even lower relaxation rates.

In summary, we report on the discovery of an alloy with the lowest intrinsic relaxation rate, $G \sim 35 \pm 5$ MHz yet observed in ferromagnetic metals. The results meet a critical need in metallic ferromagnetic materials, helping to enable high- Q integrated microwave devices and emerging devices based on spin momentum transfer.

We thank L. Berger, M. Fähnle, B. Heinrich, O. Myrasov, M. Stiles, and A. Rebei for discussions. This work was supported by the U.S. Army Research Office under Contracts No. DA-ARO-W911NF0410168, No. DAAD19-02-1-0375, and No. 43986-MS-YIP, the NSF under Grant No. DMR-02-39724, and has used the shared experimental facilities that are supported primarily by the MRSEC program of the National Science Foundation under No. NSF-DMR-0213574.

*Electronic address: web54@columbia.edu

- [1] M. Buess *et al.*, Phys. Rev. Lett. **93**, 077207 (2004).
- [2] T. Gerrits *et al.*, Nature (London) **418**, 509 (2002).
- [3] S. Kaka and S. Russek, Appl. Phys. Lett. **80**, 2958 (2002).
- [4] B. Koopmans *et al.*, Phys. Rev. Lett. **95**, 267207 (2005).
- [5] Y. Acremann *et al.*, Nature (London) **414**, 51 (2001).
- [6] W. Rippard *et al.*, Phys. Rev. Lett. **92**, 027201 (2004); I. Krivorotov *et al.*, Science **307**, 228 (2005); S. Kaka *et al.*, Nature (London) **437**, 389 (2005).
- [7] B. Heinrich *et al.*, J. Appl. Phys. **50**, 7726 (1979); **63**, 3863 (1988); IEEE Trans. Magn. **38**, 2496 (2002); Phys. Rev. Lett. **90**, 187601 (2003); J. Appl. Phys. **95**, 7462 (2004); *Ultrathin Magnetic Structures: Fundamentals of Nanomagnetism* (Springer, New York, 2005), Vol. 3, Chap. 5, pp. 143–210.
- [8] V. Kamberský, Can. J. Phys. **48**, 2906 (1970); J. Kunes and V. Kamberský, Phys. Rev. B **65**, 212411 (2002); M. Fähnle and D. Steiauf, Phys. Rev. B **72**, 064450 (2005).
- [9] J. Ho, F. Khanna, and B. Choi, Phys. Rev. Lett. **92**, 097601 (2004); A. Rebei and M. Simionato, Phys. Rev. B **71**, 174415 (2005).
- [10] Y. Tserkovnyak *et al.*, Rev. Mod. Phys. **77**, 1375 (2005).
- [11] W. Bailey *et al.*, IEEE Trans. Magn. **37**, 1749 (2001); S. Reidy, L. Cheng, and W. Bailey, Appl. Phys. Lett. **82**, 1254 (2003); A. Rebei and J. Hohlfield, Phys. Rev. Lett. **97**, 117601 (2006).
- [12] J. Slonczewski, J. Magn. Magn. Mater. **195**, 261 (1999).
- [13] C. Scheck, L. Cheng, and W. Bailey, Appl. Phys. Lett. **88**, 252510 (2006).
- [14] N. Smith and P. Arnett, Appl. Phys. Lett. **78**, 1448 (2001).
- [15] S. Bhagat and P. Lubitz, Phys. Rev. B **10**, 179 (1974).
- [16] Z. Frait and D. Fraitova, J. Magn. Magn. Mater. **15–18**, 1081 (1980); F. Schreiber *et al.*, Solid State Commun. **93**, 965 (1995).
- [17] R. A. de Groot *et al.*, Phys. Rev. Lett. **50**, 2024 (1983).
- [18] R. Hall, J. Appl. Phys. **31**, 1037 (1960); D. Johnson, F. Pinski, and J. Staunton, J. Appl. Phys. **61**, 3715 (1987); B. Drittler *et al.*, Phys. Rev. B **40**, 8203 (1989).
- [19] M. Farle, Rep. Prog. Phys. **61**, 755 (1998).
- [20] Y. Guan and W. Bailey, J. Appl. Phys. (to be published).
- [21] P. Lubitz, S. F. Cheng, and F. Rachford, J. Appl. Phys. **93**, 8283 (2003).
- [22] V. Safonov and H. Bertram, J. Appl. Phys. **94**, 529 (2003).
- [23] E. Francisco and L. Pueyo, Phys. Rev. A **36**, 1978 (1987).
- [24] G. G. Scott and H. W. Sturmer, Phys. Rev. **184**, 490 (1969).
- [25] H. Suhl, IEEE Trans. Magn. **34**, 1834 (1998).
- [26] E. Rossi, O. Heinonen, and A. MacDonald, Phys. Rev. B **72**, 174412 (2005).